FLUCTUATION OF RECENT LARGE IMPACT CRATERS RATE ON MARS FROM AUTOMATIC CRATER DETECTION A. Lagain[1], M.A. Kreslavsky[2], G.K Benedix[1], D. Baratoux[3], P. Bland[1], M. Towner[1]. J. Paxman[4], S. Bouley[5], C. Norman[1], S. Anderson[1], K. Servis[1,6], E. Samson[1], K. Chai[7] and S. Meka[7], [1]Space Science and Technology Centre, School of Earth and Planetary Sciences, Curtin University, Perth, WA, Australia (anthony.lagain@curtin.edu.au), [2]Earth and Planetary Sciences, University of California, Santa Cruz, CA, USA, [3]French Research Institute for Sustainable Development, Toulouse, France, [4]School of Civil and Mechanical Engineering, Curtin University, Perth, WA, Australia, [5]GEOPS laboratory, Paris-Saclay University, France, [6]CSIRO - Pawsey Supercomputing Centre, Kensington WA, Australia, [7]Curtin Institution of Computation, Curtin University, Perth, WA, Australia.

Introduction: Knowledge of collision rates through time and space is essential because meteoritic impact crater counting is the only way to determine the ages of surface geological units and processes on the solid bodies of our Solar System. All chronology models assume a constant size distribution of impactors and an exponential decay of the impact flux between 4 Ga and 2.5 Ga before the present followed by a constant rate over the last 2.5 Ga [1,2,3]. These two assumptions are challenged by recent evidence for an increase of the impact flux on the Moon and the Earth [5,6,7,8] and probably on Mars [9] associated with a decoupling between the flux of small and large impactors over the last billion years [8,9]. Here, using the results of an automatic crater detection algorithm [10], we investigate the evolution of the rate of formation of large impact craters ($D_c \geq 20$km) on Mars and thus infer the evolution of the flux of large impactors ($D_i >$ 5km) from the size-frequency distribution of small craters superposed to the ejecta blankets of large ones.

Automatic crater detection: The crater counting technique requires a tedious mapping and morphological inspection of a large number of impact craters. We designed and implemented a new Crater Detection Algorithm (CDA) [10] trained on the THEMIS Day-IR global mosaic [11] using the largest available crater database [12]. The objective was to map all impact craters on the Martian surface down to around 100 m in diameter. We applied our algorithm on the CTX mosaic (5m/px) [13] between ±45° of latitudes covering more than 70% of the entire Martian surface, and detected around 17 million of impact structures >50m [14]. A non-negligible part of these detections are secondary craters. To account for these, we developed a Secondary craters Clusters Identification Algorithm (SCIA) using cluster analysis statistical analyses, inspired from existing techniques [15,16,17]. We validated the results against manual counting. The newly built database of impact craters, with expected secondary craters removed, is amenable to dating any geological structures having shaped the surface of Mars at different spatial scales, including large impact craters.

Selection and dating of large craters on Mars: The dating of large impact craters on Mars is limited by several factors such as the degradation of ejecta blankets and the retention rate of small craters superposed to their ejecta. To avoid measuring the ages of post-impact resurfacing processes, that are especially active north of 35°N and south of 35°S [17], we focused on craters ≥20km in diameter exhibiting an ejecta blanket according to the crater database [12] and located on a latitudinal band between ±35°. With these criteria, we extracted a set of 2307 craters. From this population, we then extracted those where the ejecta is not affected by volcanic/tectonic processes or by the formation of another large nearby impact crater. The remaining population is assumed to have retained a sufficient number of small craters on their ejecta thus allowing formation age to be dated. The final set includes 590 impact craters.

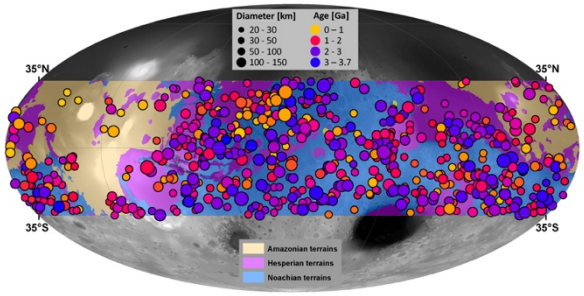

Figure 1: *Distribution of the 590 dated impact craters with D≥20km between ±35° of latitudes, scaled by size and color coded according to age, with chronostratigraphic surfaces [18].*

Among the 590 craters considered in this study, the ejecta blankets of 177 of them have been already mapped in up-to-date versions of the geological maps of Mars [18]. The ejecta of the remaining 413 craters have been mapped here. We exclude the crater and the rim from the counting area in order to further avoid any contamination of ages by surfaces recently affected by aeolian transport, or gravitationally-driven mass movements. The images comprising the uncontrolled CTX mosaic [13] sometimes exhibit artefacts, or strips of moderate quality due to atmospheric and surface conditions when an image is acquired, thus decreasing the crater detection rate. We performed manual and visual inspections of the mosaic quality over the counting area associated with each large crater in order to

identify and remove low-quality images. Regions of secondary craters clusters have also been removed from the counting area using the SCIA. Location and ages of craters dated in this study are shown on Figure 1.

Completeness of the impact rate record: If one can argue the impact cratering flux cannot be fully recorded for the last 4Ga due to resurfacing processes erasing progressively the ejecta blanket and large craters themselves, Hesperian and Noachian terrains within the 35° latitudinal band (45% of the total Martian surface) should nevertheless have retained all D>20km craters over the last billion years. The Crater-Size Frequency Distribution (CSFD) shown on Figure 2 correspond to craters younger than 600Ma superposed to these terrains and is consistent with the 600Ma isochron. This observation strongly supports the fact that the entire population of craters larger than 20km in diameter formed over the last 600 million years on this portion of the Martian surface has been counted completely. We therefore focused on the analysis of the impact rate evolution over this range of time from this crater sub-sample.

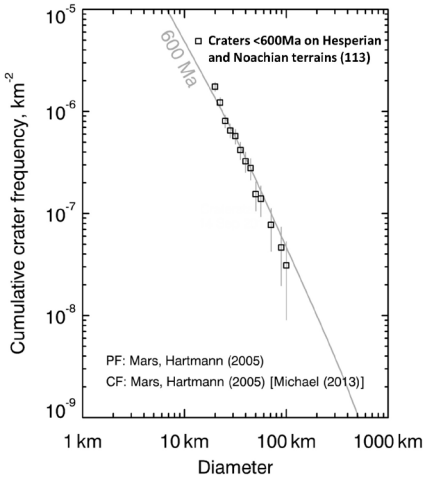

Figure 2: *CSFDs of impact craters considered in this study. Black CSFD correspond to craters located on Hesperian and Noachian terrains, for which the model age is less than 600Ma. This CSFD is consistent with the number of craters expected on a terrain aged of 600Ma with the same size than Hesperian and Noachian terrains [1,18].*

Impact cratering rate evolution: Figure 3 shows the relative impact cratering flux obtained from the summation of probability density functions of impact crater ages from the crater sub-sample. The formation of large impact craters is not homogeneously distributed over the time range investigated here. Our data suggest an inconsistency between the flux used to date each crater and the rate inferred from these datings, thus implying that the small and large body impact fluxes are decoupled from one another, confirming results from [6,9]. We note also sharp peaks centered around 480, 280 and 100Ma. Preliminary statistical test show that 280Ma peak is marginally significant whereas the two others are too small to be statistically significant. This pattern would be consistent with other independent arguments for increased rate with similar intensity and timing on the Moon and Mars [5,6,7,8] for which the causes are probably collisions and potentially formation of asteroid families within the main asteroid belt.

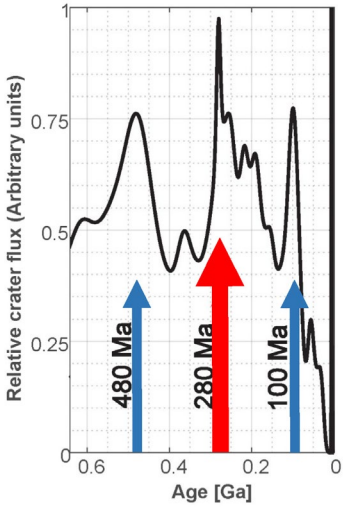

Figure 3: *Relative impact cratering rate distribution from craters younger than 600Ma superposed on Hesperian and Noachian terrains.*

References: [1] Hartmann, W.K. (2005) *Icarus*, 174, 294-320. [2] Neukum, G.G. (2001) *Space Sci. Rev.*, 96, 55-86. [3] Hartmann, W.K. & Neukum, G.G. (2001) *Sp. Sci. Rev.* 96, 165-194. [4] Bottke, W.F. et al. (2015) *Asteroids IV* 701-724. [5] Martin, E. et al. (2018) *Met. & Pl. Sci*. 53, 2541-2557. [6] Mazrouei, S. et al. (2019) Science, 363, 253-257. [7] Schmitz, B. et al. (2019) *Sci. Adv.*, 5, eaax4184. [8] Vokrouhlický, D. et al. (2017) *Astron. J.* 23pp, 172. [9] Lagain, A. et al. (2020) *PSS*, 180, 104755. [10] Benedix, G.K. et al. submitted to *Earth and Space Science* (19 Nov. 2019). [11] Edwards, C. et al. (2011) *JGR*, 116(E10). [12] Robbins, S. & Hynek, B.M. (2012) *JGR* 117(E6001). [13] NASA/JPL/MSSS/The Murray Lab. [14] Lagain, A. et al. (2020) 51st LPSC. [15] Andronov, L. et al. (2016) *Nature, Sci. Reports*, 6, 2045-2322. [16] Salih, A.L. et al. (2017) *Int. Arch. Photogramm. Remote Sens. Spatial Inf. Sci.*, XLII-3/W1, 125-132. [17] Kreslavsky, M. & Head III, J.W. *GRL*, 45. [18] Tanaka, K.L. et al. (2014) Geologic map of Mars, *U.S.G.S. Scientific Investigations Map 3292*.

Acknowledgement: This work is supported by the resources provided by the Pawsey Supercomputing Centre with funding from the Australian Government, Curtin University, and the Government of Western Australia.